THE MICROASAR EXPERIMENT ON CASIE-09

David G. Long, Evan Zaugg, Matthew Edwards, and James Maslanik

***Abstract*—During the summer of 2009, the Characterization of Arctic Sea Ice Experiment 2009 (CASIE-09) operated a small, unmanned aircraft system (UAS) over the Arctic Ocean for a number of long-distance flights from Svalbard Island. In addition to other instruments, the UAS carried a small C-band synthetic aperture radar (SAR) known as MicroASAR to image sea ice roughness at 1 m resolution. This paper briefly describes the SAR, its role in CASIE-09, and presents sample SAR image results.**

***Index Terms*—sea ice, synthetic aperture radar, UAS**

I. Introduction

In July 2009, a small, low power SAR was flown on a medium-sized, unmanned aircraft system (UAS) as part of the Characterization of Arctic Sea Ice Experiment 2009 (CASIE-09) [1] over the Arctic Ocean from Svalbard Island. The goal of the mission was to measure ice roughness in support of research into monitoring ice thickness and ice age. The C-band SAR instrument, known as MicroASAR, collected 19.8 hours of SAR image data over five UAS flights of varying length from 6-10 hours long. The UAS was the NASA Sensor Integrated Environmental Remote Research Aircraft (SIERRA) [2]. This paper briefly describes the MicroASAR, its role in CASIE-09, and presents initial SAR results.

II. MICROASAR AND THE SIERRA UAS

Synthetic aperture radar (SAR) can be a useful tool for sea ice observation, but has traditionally been large and expensive. The compact MicroASAR builds on the design of the BYU microSAR [3], but is a much more robust and flexible system [4]. The MicroASAR uses a linear frequency-modulated continuous-wave (LFM-CW) transmit signal generated by a direct digital synthesizer (DDS) chip and shifted up to C-band. The system is configured to operate in bistatic mode, so that it transmits and receives at the same time using two different antennas. This enables long transmit chips to maximize the SNR while minimizing peak transmit power. The two antennas maximize the isolation between the transmit and receive signals.

The return signal is mixed down with a frequency-shifted copy of the transmit signal (analog dechirp) followed by an all-digital final IF stage and filtering. Internal filtering further reduces the transmit/receive signal feedthrough. Raw SAR data and GPS position data are stored to a pair of compact flash (CF) disks. Using a 32 GB CF disk, over two hours of SAR data can be recorded. The MicroASAR transmit bandwidth is 160 MHz, yielding a nominal range resolution of approximately 1 m. Table 1 provides a brief summary of the MicroASAR specifications and operating characteristics.

A key goal of CASIE-09 was to provide fine spatial resolution from multiple sensors over difficult to access locations in the high Arctic. Satellites cannot provide the desired simultaneous combination of sensor types and resolution. Piloted aircraft typically fly too high and too fast to yield the fine-scale sampling rates and mapping patterns required by our project. UAS-based measurements can be made a low speed and low altitude in dangerous Arctic conditions without putting humans at risk.

In CASIE-09 the MicroASAR was flown aboard the NASA

Tab. 1. CASIE-09 MicroASAR specifications

Physical Specifications	
Transmit Power	30 dBm
Supply Power	< 35 W
Supply Voltage	+15 to +26 VDC
Dimensions	22.1x18.5x4.6 cm
Weight	2.5 kg
Radar Parameters	
Modulation Type	LFM-CW
Operating Frequency Band	C-band
Transmit Center Frequency	5428.76 MHz
Signal Bandwidth	80-200 MHz (variable)
PRF	7-14 kHz (variable)
Radar Operating Specifications	
Theoretical Resolution	0.75 m (@ 200 MHz BW)
Operating Altitude	500-3000 ft
Max. Swath Width	300-2500 m (alt. dependent)
Operating Velocity	10-150 m/s
Collection Time (for 10GB)	30-60 min (PRF dependent)
Antennas (2 required)	
Type	2 x 8 Patch Array
Gain	15.5 dB
Beamwidth	8.5°x50°
Size	35x12x0.25 cm

D. G. Long is with the Electrical and Computer Engineering Department, Brigham Young University, Provo, UT 84602 USA (phone: 801-422-4383; e-mail: long@ee.byu.edu).

Evan Zaugg and Matthew Edwards are with Artemis, Inc., Hauppauge, NY, USA. (e-mail: evan @artemis.net; matt@artemisinc.net).

James Maslanik is with the Electrical Engineering Department, University of Colorado, Boulder, CO 80309 USA (e-mail: james.maslanik@colorado.edu).

SIERRA UAS [2]. With a relatively large payload capacity, (25 kg.), medium size (6m wingspan), efficient mission planning software, and an in-flight programmable autopilot, the SIERRA is well-suited for the long-duration missions used in the CASIE-09 experiment. Some of the other sensors on the UAS included two optical cameras, two pyrometers, a up/down-looking shortwave spectrometer, high-quality inertial measurement unit (IMU), and a laser profilometer system consisting of two down-pointing lasers, a medium-quality IMU, and differential-capable GPS receiver [4, 5]. The UAS provided GPS position data to the MicroASAR where it was included in the SAR processing stream. A video camera was mounted to view in the same direction as the MicroASAR, providing optical imagery coincident with the SAR swath. The UAS was flown at a low altitude (typically between 185 m and 450 m). This altitude range supports both profilometer and SAR operation. While the low altitude limits the MicroASAR swath width and results in a broad range of incidence angles, it benefits the SAR measurement SNR and noise equivalent radar backscatter. The broad incidence angle can be exploited to better understand scattering mechanisms from ice.

The UAS flights originated from Ny-Alesund, Svalbard, Norway, providing an acceptable flight range to the sea ice pack within Fram Strait to the west (see Fig. 1). Ny-Alesund offers relatively close access to sea ice pack containing a range of thicknesses, age, and ridging characteristics. Sea ice in Fram Strait is transported from the central Arctic Ocean, thus providing an opportunity to sample a variety of ice types ranging from first-year ice to ice that is several years old [6]. Five science flights covering 2923 km of sea ice were flown in July 2009 as part of CASIE-09. Flight planning took advantage of near real-time ice imaging from QuikSCAT, ENVISAT, AMSR, MODIS and AVHRR. These proved invaluable in determining the location of the sea ice edge. Figure 1 illustrates a sample near real-time QuikSCAT image like those used for flight planning. This image was viewed in Google Earth with track data overlaid. The goal was to ensure flights over the ice edge and variety of ice conditions while optimizing the ground track for the various sensors carried aboard the UAS. Race-track and intersecting straight flight paths were used to obtain observations of selected areas at multiple incidence angles and with multiple sensors.

III. SAR Images

Raw MicroASAR data collected during the flight and stored on-board was post-processed into SAR images using both the Range Doppler Algorithm (RDA) and the Frequency Scaling Algorithm (FSA), a version of the Chirp Scaling Algorithm (CSA) adapted for LFM-CW SAR operation. Images have also been processed using the backprojection algorithm. Azimuth resolution after multi-looking is 0.5 m. The range resolution is 1 m. While post-processing of collected GPS data improves position information, limitations in the motion measurement preclude applying full motion compensation [5],

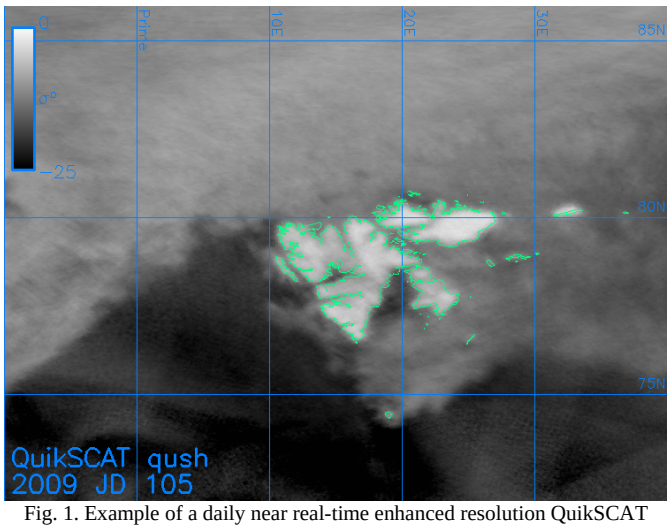

Fig. 1. Example of a daily near real-time enhanced resolution QuikSCAT image used for navigation planning and data mapping during CASIE-09. The pixel resolution is 2.225 km. Ny-Alesund is near the upper left of Svalbard Island in the center of the image. The Fram Strait is on the left.

but the smooth flight of the SIERRA UAS enables production of well-focused images. Figure 2 illustrates the deviation from an ideal straight-flight for a typical 100 s image segment.

Raw SAR data collected by the MicroASAR was divided into 1 min segments and separately processed into multi-looked image segments typically 3.5 km long in the along-track dimension by 1.2 km wide in the cross-track dimension. The processed SAR images show a variety of surface features, from open ocean to dense pack ice. Features visible in the SAR imagery, as confirmed by the corresponding video, include ridges, rubble fields, brash ice, leads, and melt ponds. Sample MicroASAR images illustrating some of these features are shown in Figs. 3, 4, and 5. Creation of .kmz files enables convenient browsing in Google Earth. Flight tracks were specified to provide overlapping SAR imaging swaths (see Fig. 4) with overlapping laser profilometer tracks.

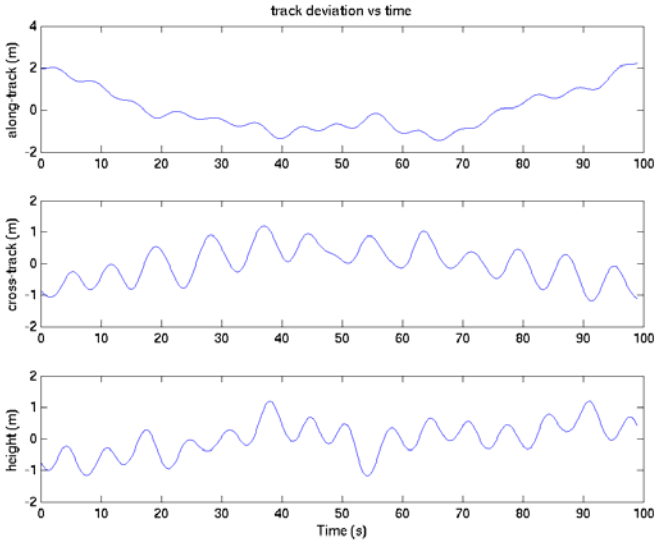

Fig. 2. Plots of the UAS displacement from ideal straight-line flight for a typical image during CASIE09 flights. The periodic variation is due to the UAS autopilot operation.

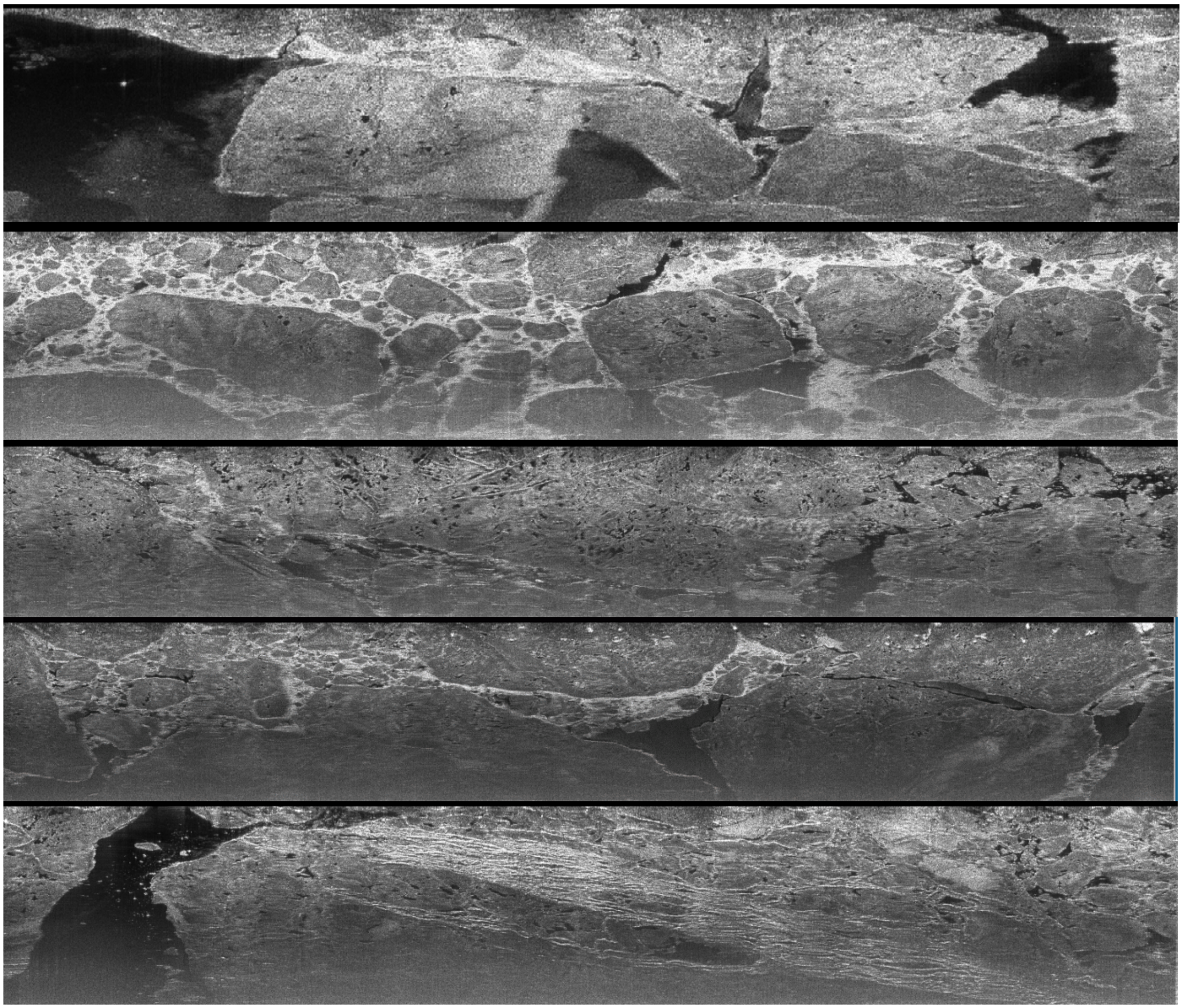

Fig. 3. Sample georectified MicroASAR images collected from two different flights during from CASIE-09 illustrating a number of different sea ice features. Nadir is along the top of each image. The UAS flew from left to right. The incidence angle varies from zero at the top to over 60 deg as the bottom of the image. The image dimensions are approximately 3.5 km by 1 km. The multi-looked pixel resolution is 0.5 m in azimuth by 1 m in range.

The SAR imagery compares well to the simultaneous optical imagery, see Fig. 5. Both optical and MicroASAR images are being compared to spaceborne radiometer and scatterometer observations to better understand the relationship between roughness and ice conditions during the summer ice melt period. The MicroASAR image data set includes overlapping images with a wide range of incidence angle, to help understand the scattering mechanisms of the features observed.

IV. Conclusion

The CASIE-09 experiment has demonstrated the practicality of a small SAR on a UAS for studying sea ice in the Arctic. Coupled with data from other on-board instruments and spaceborne sensors, MicroASAR images are expected to expand our understanding of small-scale sea ice roughness.

Acknowledgment

We thank the CASIE-09 experiment team, the Norwegian Polar Institute, and all those who assisted for their effort and support to make this experiment a resounding success. We also thank the numerous data centers and organizations for provision of satellite imagery.

References

[1] J. A. Maslanik, R .I. Crocker, K. Wegrzyn, C. Fowler, U. C. Herzfeld, D. Long, R. Kwok, M M Fladeland, P. Bui, G. Bland, “Characterization of Fram Strait Sea Ice Conditions Using the NASA SIERRA Unmanned Aircraft System,” AGU Fall Meeting 2009, San Francisco, CA, abstract C43D-06.

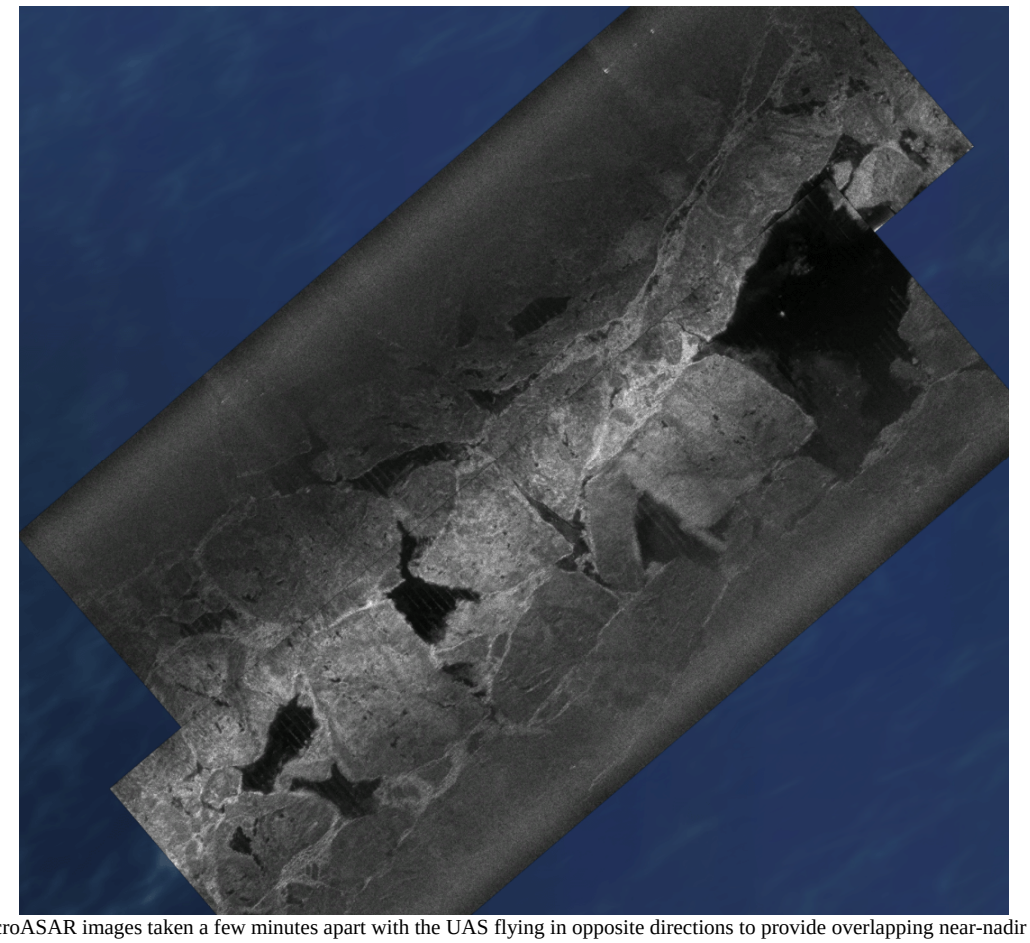

Fig. 4. Two MicroASAR images taken a few minutes apart with the UAS flying in opposite directions to provide overlapping near-nadir swath coverage.

[2] M.M. Fladeland, R. Berthold, L. Monforton, R. Kolyer, B. Lobitz, and M. Sumich, "The NASA SIERRA UAV: A new unmanned aircraft for Earth science investigations," AGU Fall Meeting 2008, abstract B41A-0365.

[3] E.C. Zaugg, D.L. Hudson, and D.G. Long, "The BYU microSAR: A Small, Student-Built SAR for UAV Operation," *Proc. Int. Geosci. Rem. Sen. Symp*., Denver, Colorado, pp. 411-414, Aug. 2006.

[4] E.I Crocker, J.A. Maslanik, S.E. Palo, C. Fowler, U.C. Herzfeld, and W.J. Emery, "A Sensor Package for Ice Surface Characterization Using Small Unmanned Aircraft Systems," *IEEE Trans. Geosci. and Remote Sensing*, submitted.

[5] M. Edwards, D. Madsen, C. Stringham, A. Margulis, and B. Wicks, "MicroASAR: A Small, Robust LFM-CW SAR for Operation on UAVs and Small Aircraft," in *Proc. Int. Geosci. Rem. Sen. Symp.*, Boston, Mass, pp. 514-517, July, 2008.

[6] R. Kwok, and D. A. Rothrock, "Variability of Fram Strait Ice Flux and North Atlantic Oscillation," *J. Geophys. Res.*, Vol. 103, No. C4, pp. 8191-8214, 1998.

[7] E.C. Zaugg and D.G. Long, "Theory and Application of Motion Compensation for LFM-CW SAR," *IEEE Trans. Geosci. and Remote Sensing*, Vol. 46, No. 10, pp. 2990-2998, 2008.

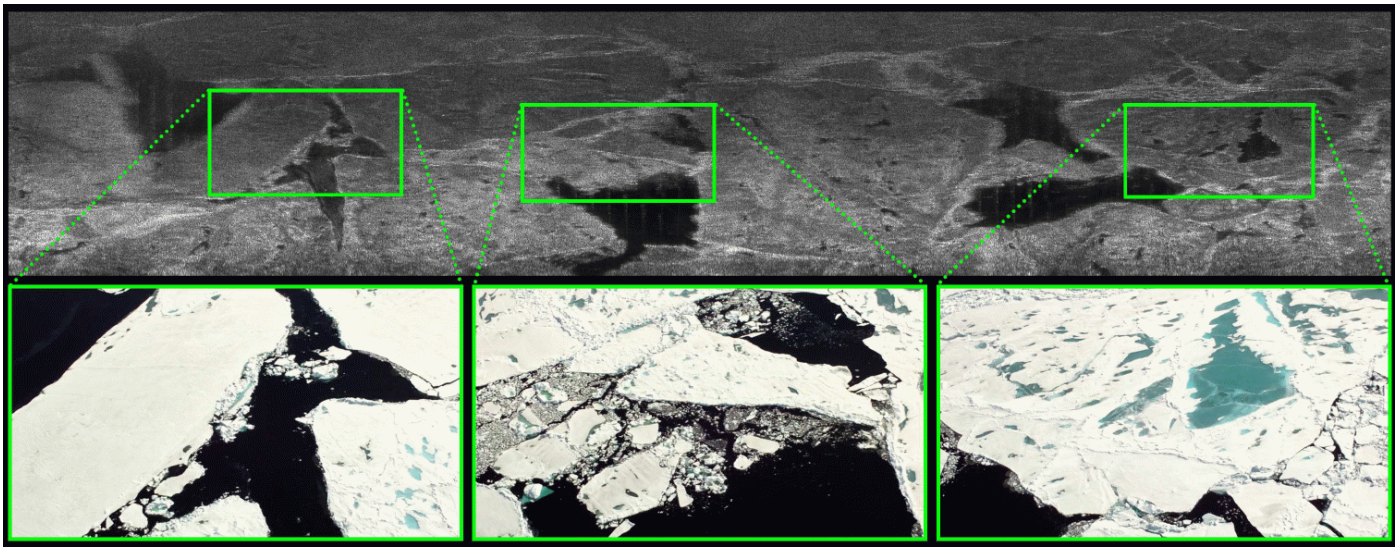

Fig. 5. Comparison of features in the optical video and a slant-range MicroASAR image from CASIE-09. Nadir is along the top of the MicroASAR image.